Nuclear Materials and Energy 37 (2023) 101543

Contents lists available at ScienceDirect

Nuclear Materials and Energy

journal homepage: www.elsevier.com/locate/nme

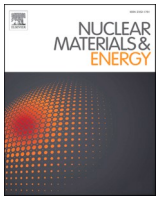

LIBS plasma in atmospheric pressure argon, nitrogen and helium: Spatio-temporal distribution of plume emission and H_α linewidth

Indrek Jõgi [a,*], Jasper Ristkok [a], Jelena Butikova [b], Jüri Raud [a], Peeter Paris [a]

[a] Institute of Physics, University of Tartu, Tartu 50411, Estonia
[b] Institute of Solid State Physics, University of Latvia, Riga LV-1063, Latvia

ARTICLE INFO

Keywords:
Laser Induced Breakdown Spectroscopy
Fuel retention
Hydrogen isotope determination
Laser induced plasma plume

ABSTRACT

Laser Induced Breakdown Spectroscopy (LIBS) method is considered for assessing the retention of hydrogen isotopes in the ITER plasma-facing components during the maintenance breaks when the reactor is filled with near atmospheric pressure nitrogen or inert gas. At these conditions, the broadening of the spectral lines of hydrogen isotopes and the reduction of line intensities complicates the distinguishing of hydrogen isotopes. The aim of the present study was to investigate the effect of atmospheric pressure nitrogen, argon and helium ambient gas on the spatio-temporal distribution of the LIBS plasma plume emission and linewidths of H_α line, representing the hydrogen isotopes. Nd:YAG laser with 8 ns pulse width was used to ablate the molybdenum (Mo) target with hydrogen impurity. The development of the formed plasma plume was investigated by time and space-resolved emission spectra in the 20 nm range around the 656.28 nm H_α line. For all gases used in the experiments, the intensity and linewidth of H_α line decreased with the delay time between the laser pulse and the spectral registration. At the same linewidth values, the highest intensities were obtained in the helium atmosphere while the lowest intensity was obtained in nitrogen. According to spatially resolved spectral measurements, the H_α line was most intense near the Mo target while the Mo lines peaked farther away. In the case of the helium atmosphere, the plasma plume emission was observed at a longer distance from the target and it decayed faster than in argon and nitrogen atmospheres. According to these results, helium is the most beneficial ambient gas for hydrogen isotope detection by atmospheric pressure LIBS. The use of argon ambient gas may be required when LIBS is used for the simultaneous determination of fuel and He retention in the wall material.

1. Introduction

Retention of fuel, hydrogen isotopes deuterium and tritium, in the first wall and divertor of fusion reactors like ITER is a severe problem that has to be solved before the successful utilization of fusion energy [1]. As one step in measuring the amount of retained fuel, it is necessary to develop diagnostic methods suitable for the in-vessel fuel retention measurements. Laser Induced Breakdown Spectroscopy (LIBS) method is considered for the hydrogen isotope measurements in the first wall and divertor of ITER during the maintenance phase when the vacuum vessel is filled with near atmospheric pressure nitrogen or inert gas [2]. LIBS uses short intense laser pulses to ablate, evaporate and ionize the wall material into a transient plasma plume. The optical emission of the excited elements is then recorded by a spectrometer. Distinguishing between different hydrogen isotopes is complicated because of the proximity of the emission lines: 656.04, 656.10 and 656.28 nm for tritium (T), deuterium (D) and hydrogen (H) Balmer alpha lines, respectively. The plasma densities encountered in the laser-induced plasma plume will cause considerable Stark broadening of hydrogen isotope lines, especially at atmospheric pressures [3,4]. The broadening may even reach values above 1 nm at the initial stages of the plasma plume development which complicates the distinguishing of isotopes [3,5]. At later stages, the plasma density and correspondingly the emission linewidth and intensity decrease [5].

Our earlier LIBS studies in atmospheric pressure argon (Ar) and nitrogen (N_2) mixtures showed an exponential decrease of H_α line intensity with the increasing delay time between the laser pulse and registration of the spectrum [5]. The intensity decreased considerably faster in the presence of nitrogen in the gas mixture but for both gases and for all delay times, the H_α linewidth remained above 0.18 nm which is larger than the wavelength difference between deuterium and hydrogen lines or deuterium and tritium lines. Several studies have

* Corresponding author.
E-mail address: Indrek.jogi@ut.ee (I. Jõgi).

https://doi.org/10.1016/j.nme.2023.101543
Received 15 August 2023; Received in revised form 9 October 2023; Accepted 25 October 2023
Available online 29 October 2023

shown that the use of helium (He) atmosphere results in lower electron densities and electron temperatures when compared to Ar or air [6–10]. As the Stark broadening of the emission lines depends on the plasma density, using He background gas, may potentially result in sufficiently strong line intensities at narrower hydrogen isotope linewidths. However, systematic studies investigating the effect of He background gas on the H_α line intensity and linewidth are still missing.

Another observation of our previous paper which investigated the LIBS in Ar-N_2 mixtures was the difference in the spatial distribution of the total plume emission and emission at a narrow wavelength range around the H_α line [5]. The latter was stronger near the target when compared to the total emission. The spatial variation of the distribution of emission intensities and plasma parameters reduces the applicability of the calibration-free LIBS method [11–13], which is required for the quantitative analysis of sample composition and hydrogen isotope retention [2]. In our previous study, we used an interference filter that did not allow discrimination between H_α line and background emission. A more precise distribution of the emission of different elements could be achieved by recording the spatially resolved spectra.

The aim of the present study was to compare the spatial and temporal changes of H_α 652.28 nm line and Mo lines of laser-induced plasma plume in the atmospheric pressure Ar, N_2 and He. The gas atmosphere resulting in the optimal conditions for 'in situ' LIBS analysis of plasma facing materials in the reactor vessel can be obtained by flushing the ambient environment with the desired gas [2,14,15]. As a note, it has been shown that, while H and D have different spatial distributions at lower pressures [16], all hydrogen isotopes and their emission lines have expectedly similar behavior in the plasma plume at atmospheric pressure. Therefore, the time-dependence of H_α line intensity and FWHM can be considered to be representative also for other hydrogen isotopes.

2. Experimental setup

The LIBS system depicted in Fig. 1 is similar to the one used in our previous studies [5,17]. Quantel Nd:YAG laser generated at the second harmonic at 532 nm wavelength, the pulse width was 8 ns. The laser beam was focused normally on the target surface. The laser pulse energy was 60 mJ and the corresponding fluence at the target surface was approximately 15 J/cm^2. The target was a molybdenum disc with a diameter of 30 mm and thickness of 2.5 mm. The molybdenum contains about 0.5 at. % of hydrogen as an impurity as measured by Time-of-Flight Elastic Recoil Detection Analysis method in our earlier study [5]. The Mo target was placed in a vacuum chamber which allowed to control the gas atmosphere (N_2, Ar or He). The vacuum chamber was initially evacuated with an oil rotary pump to the pressure of 10^{-3} mBar or better and then filled with the desired gas to the pressure of 1 bar from the gas cylinders of argon, nitrogen or helium with purity class 5.0 (<0.001 % impurities). The pressure in the chamber was measured with MKS DualTrans^{TM} 910 Transducer. All LIBS experiments were made at static pressures of 1 bar.

The emission spectra were collected with two different configurations. The first configuration collected the emitted spectra at 45 degrees. The details of this configuration are described in our paper [5] and are briefly repeated here. A quartz lens was used to produce a reduced 1:3 image of the plasma plume. This allowed us to obtain strong signal at the cost of spatial resolution. The round end of the round-to-linear fiber bundle with diameter of 0.8 mm was placed to the image plane. The other end of the fiber was placed at the slit of the 0.5 m Czerny-Turner type spectrometer (MDR-63, grating 1200 grooves/mm) coupled with Andor iStar 340 T ICCD camera. The spectrometer with the spectral resolution of 0.07 nm (FWHM determined by He-Ne laser at 632.8 nm) collected spectrum in the wavelength range of 20 nm centered around H_α line at 656.28 nm. The delay time between the laser pulse and spectral recording was varied between 0.4 and 12 μs. The gate width was fixed at 200 ns. For each experimental condition, five spectra were accumulated from one spot on the target and each new experiment started at a new location. Previous measurements showed that the variation of H_α line intensities registered at different areas on the surface remained within 10 % [5].

The second configuration collected the emitted spectra perpendicularly with the plume development axis. The magnification used in this configuration was nearly 1:1 and the registered line intensities were therefore weaker. The position of the optical fiber was shifted along the axis of the plume image. This allowed the investigation of spatially resolved development of emission line intensities, plasma temperature and electron density. The rest of the spectral recording system remained essentially the same as used in the first configuration. In this configuration, three spectra were accumulated for improved signal to noise ratio, the gate width was 200 ns for delay times up to 1.2 μs and it was increased up to 1 μs for longer delay times. The measurements were conducted at a single spot for each gas and the first two shots at the fresh surface were used for the cleaning of the surface and corresponding

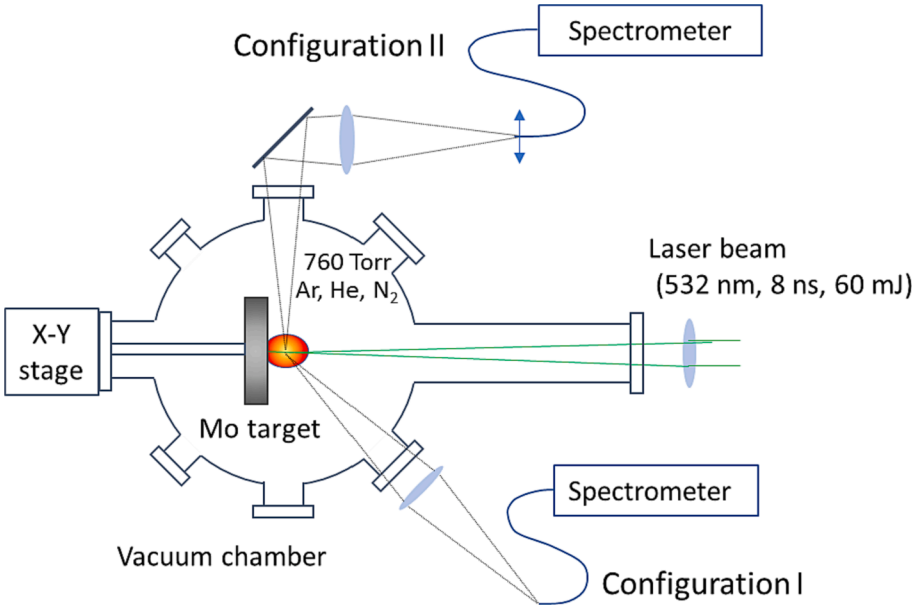

Fig. 1. Schematic description of the LIBS measurement setup.

spectra were not recorded [4].

3. Results and discussion

3.1. Temporal development of spatially integrated plasma plume emission

LIBS emission spectra of H_α line recorded at the delay time of 1, 4 and 1.2 μs respectively in He, Ar and N_2 atmosphere are shown in Fig. 2. The linewidths and intensities depended strongly on the used atmosphere. It is apparent, that the N_2 atmosphere resulted in the broadest and He atmosphere in the narrowest line when the amplitude values of the lines were comparable. For most of the delay times used, the width of the H_α line was determined by Stark broadening and the line was therefore fitted with Lorentz function. The fitting allowed us to determine both the peak area (intensity) and the FWHM of the peak. The latter was used to calculate the electron density according to the tabulated data by Gigosos et al. [18]. The width of recorded Mo lines was mainly determined by the apparatus function of the spectrometer (0.07 nm) and the line was fitted with Gaussian functions.

The time-decay of H_α lines is shown in Fig. 3a for different gas atmospheres. The intensity decrease was fitted by an exponent and the characteristic time-constant is shown in the figure for each gas. The characteristic time-constants were comparable for He and N_2 while in Ar the intensity decrease was considerably slower. The initial intensity at short time delays was similar in Ar and N_2 while in He the intensity was always somewhat smaller.

Fig. 3b shows the decrease of FWHM values of H_α line which are determined by electron density [5,18]. The line widths were highest in Ar and smallest in He. The time dependence of the decrease of FWHM was reasonably well fitted by the power function in Ar and He but in N_2 a good fit was obtained by an exponent function.

Both the intensity and FWHM values of H_α line were lowest in He and highest in Ar. For identification and discrimination of hydrogen isotopes, it is desirable to have the highest possible intensity at FWHM values comparable to or below the wavelength difference of 0.18 nm for D and H lines and 0.06 nm for D and T lines. Fig. 4 compares the intensity as a function of FWHM for different gas atmospheres. The delay times for the same FWHM values vary for different gases. It is evident that at the same FWHM value, the use of He atmosphere results in the highest intensity values. Reasonably high signal to noise values were obtained even at FWHM values below 0.18 nm which shows that He is the most favorable gas for LIBS-based fuel retention measurements at atmospheric pressure conditions considering the requirement to distinguish hydrogen isotopes.

The application of the calibration-free LIBS relies on the presence of local thermodynamic equilibrium (LTE). One of the LTE conditions is the fulfillment of McWhirter criteria, which sets a lower limit of the electron density [11–13] and therefore to the FWHM values. In the present case, the required FWHM values are above 0.9 nm. Therefore, it is not possible to register one single spectrum for the separation of the hydrogen isotope lines and for the fulfillment of McWhirter criteria. The spectrum used to distinguish hydrogen isotopes and assess the relative concentration of isotopes has to be registered at long delay time and the spectrum fulfilling the McWhirter criteria for LTE has to be registered at short delay time.

3.2. Spatially resolved development of plasma plume emission and characteristics

Further studies were carried out to investigate the temporal development of the emission spectra along the axis of the plasma plume. Our previous study showed that for atmospheric pressure Ar and N_2, the intensity of the plasma plume decreased faster in N_2 but spatio-temporal development of the total emission of plasma plume was almost similar after the first 1 μs [5]. However, there were differences in the spatial distribution of emission around H_α line at 656 nm. Therefore, the spectra were recorded perpendicularly to the plume development at different distances from the target. Note that the intensities on the following figures can't be compared to previous intensities due to different experiment geometry. Fig. 5 shows examples of the spectra recorded near the target and 4 mm from the target in the case of He atmosphere. According to these results, H_α line intensity dominated near the target, while farther away from the target the H_α line intensity diminished and Mo I lines became dominant. Similar tendencies were observed in Ar and N_2 atmospheres.

Fig. 6 shows the intensities of H_α line at 656.28 nm, the intensities of the strongest Mo I line in the registered spectral range at 661.91 nm and background intensity along the plume axis for various delay times in Ar, N_2 and He. The background intensity was determined by averaging the signal in a narrow wavelength range from 651.40 nm to 651.43 nm due to the interference from various and often unidentified Mo lines and H_α line in other wavelength regions. H_α line emission originated mainly from the plume region of the first 2 mm of the target while Mo line emission increased with the distance from the target and achieved maximum value at 2–3 mm from the target, decaying at longer distances. In all gases, H_α line intensity decreased quickly with the delay time. In contrast, Mo 661.91 nm line intensity remained almost unchanged during the used delay times for Ar and N_2 and decreased in the case of He atmosphere.

H_α line intensity was considerably weaker in nitrogen where it was detectable only in the 1 mm region closest to the target and decreased very quickly reaching noise level during the first 3 μs of plasma plume

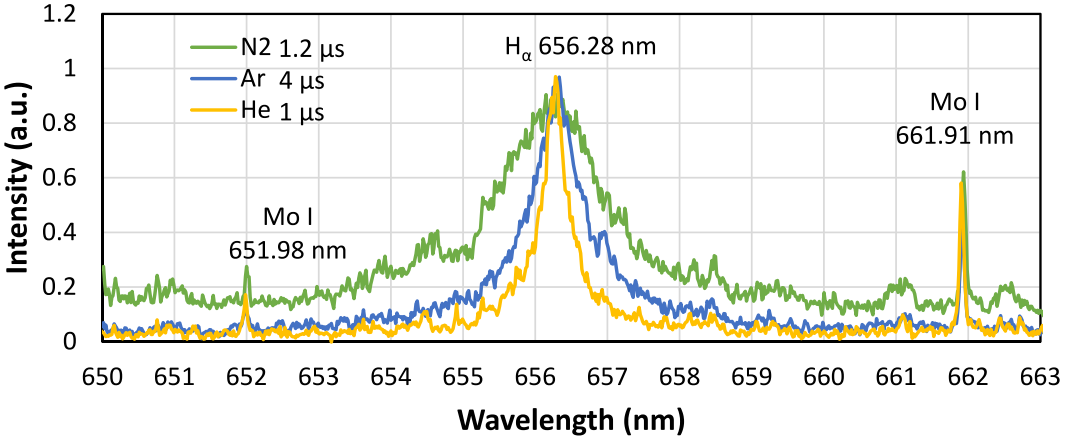

Fig. 2. Examples of LIBS emission spectra around the 656 nm H_α line were registered at different delay times for each gas to obtain approximately the same amplitude of the H_α line.

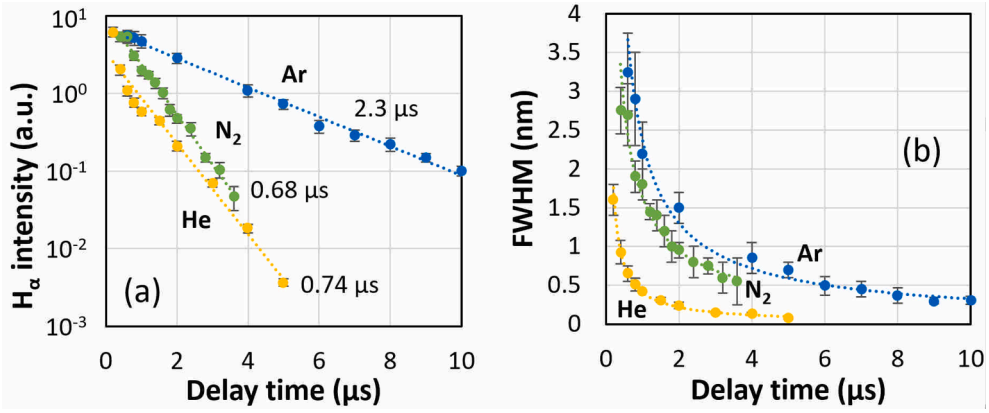

Fig. 3. H_α line intensity and the value of FWHM as the function of delay time for Ar, N_2 and He atmosphere. The time constants describing the exponential decrease of H_α intensity are also shown in Fig. 3a.

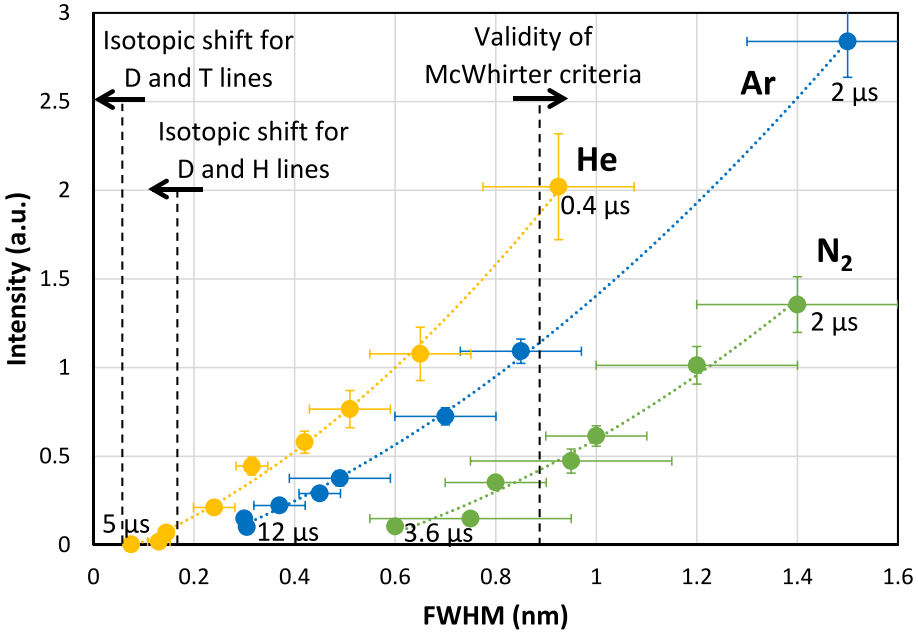

Fig. 4. H_α line intensity as a function of FWHM at varying delay times for Ar, N_2 and He atmosphere. Both line intensity and FWHM values decrease when delay times increase from 0.4 to 5 μs for He, from 2 to 12 μs for Ar and 2 to 3.6 μs for N_2 atmosphere. The figure shows that it is favorable to use He atmosphere to acquire stronger signal at low FWHM values.

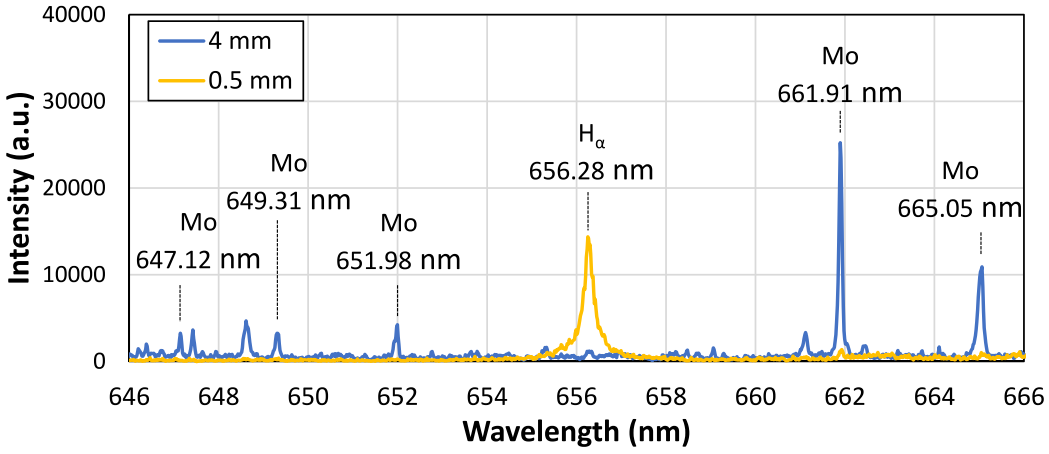

Fig. 5. Mo and H emission spectra collected perpendicularly along the plasma plume at the distance of 0.5 mm and 4 mm from the target surface in He atmosphere. The delay time was 1 μs.

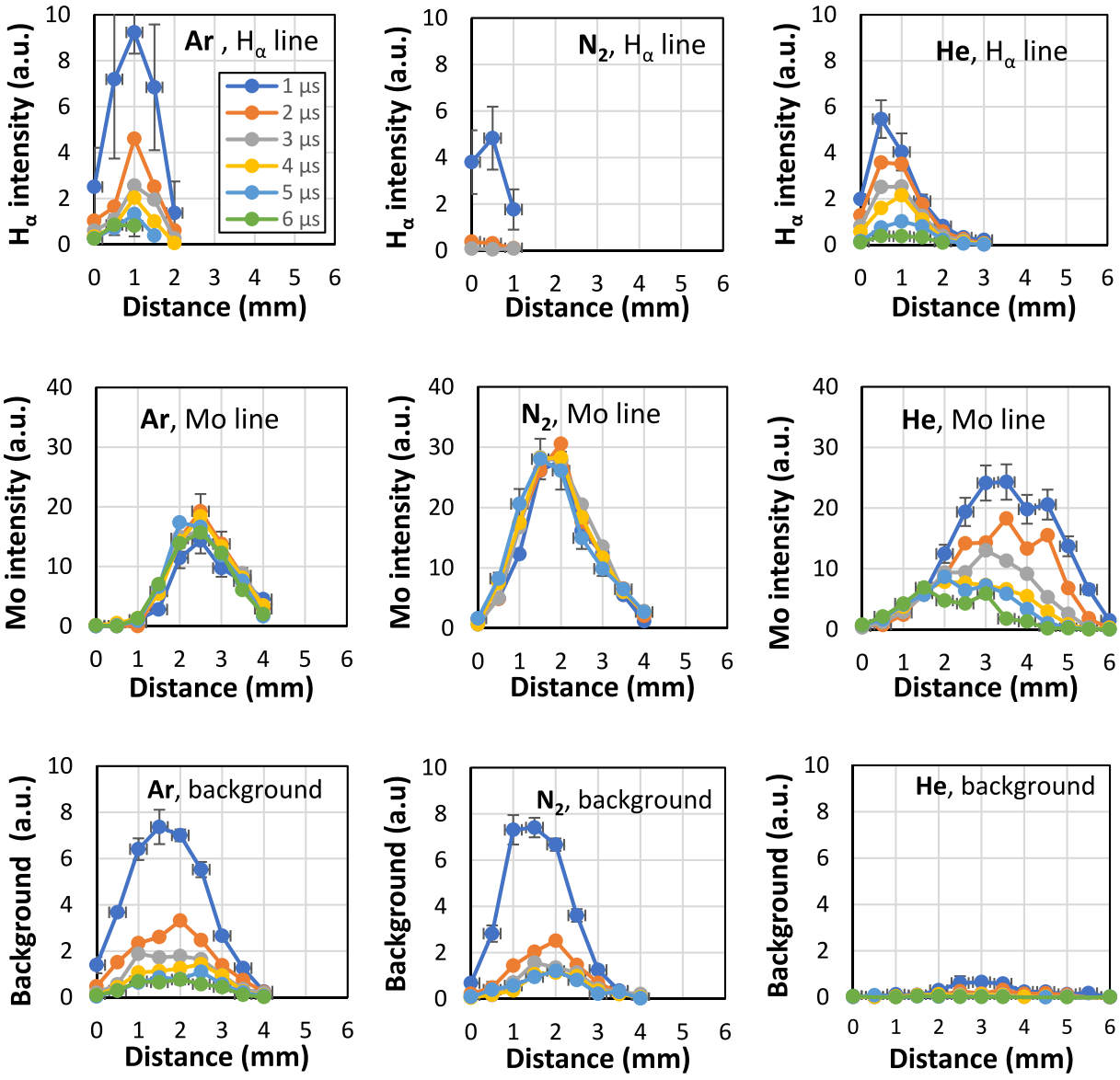

Fig. 6. The intensity of H_α line at 656.28 nm, the Mo line at 661.91 nm and background intensity as a function of distance from the target along the plume axis for different delay times in Ar, N_2 and He.

evolution (Fig. 6). The Mo 661.91 nm line intensity reached also maximum value closest to the target in nitrogen while the maximum intensity of Mo line was also the highest in nitrogen. The best signal to noise ratio and the narrowest linewidth of H_α line was obtained in He atmosphere. The total dimensions of the plume were remarkably larger in He atmosphere. Mo line intensity reached a maximum between 2 and 5 mm depending on the delay time. The farthest region where Mo could be detected in He atmosphere was 6 mm. Differently from Ar and N_2, the Mo 661.91 nm line intensity decreased and the position of Mo emission maximum shifted towards the target with delay time in He atmosphere.

The background intensity around H_α line was similar for Ar and N_2 while in the case of He atmosphere, the background intensity was approximately one order of magnitude smaller (Fig. 6). In the case of Ar and He, the background intensity peaked at the distance, which was between the intensity maximums for H_α line and Mo lines. In the case of N_2, the spatial distribution was comparable with the distribution of Mo line intensity but this may be the result of quickly diminishing H_α line intensity. Differently from Mo lines, the background intensity decreased with the delay time. Noise grows with the background intensity and therefore, the noise of H_α line was much lower in He atmosphere even at similar line intensity values. The background intensity can be attributed to the continuum emission of radiative recombination [19]. We also checked the integral intensity of the spectra recorded between 644 and 667 nm. It decreased approximately exponentially with time similarly to the total intensity of the plasma plume emission observed in the previous study [5]. This suggests that the background intensity gives an important fraction to the integral intensity of the plasma plume emission.

The differences in the development of plasma plume emission are partially similar to the results of previous studies [4]. Nearly static spatial distribution of H_α and Mo lines in Ar and N_2 atmosphere observed in the time-frame of 1–6 µs complies with the results of our previous study where the length of the plasma plume image remained practically same after 1 µs [5]. However, in He there seems to be a shift in H_α emission away and Mo emission towards the target in the observed time-frame.

The spatial and temporal changes of electron density determined from the FWHM value of H_α line were similar with the changes of H_α line intensity (Fig. 7). The electron density was highest in the first 2 mm along the plume axis and quickly diminished at longer distances and it

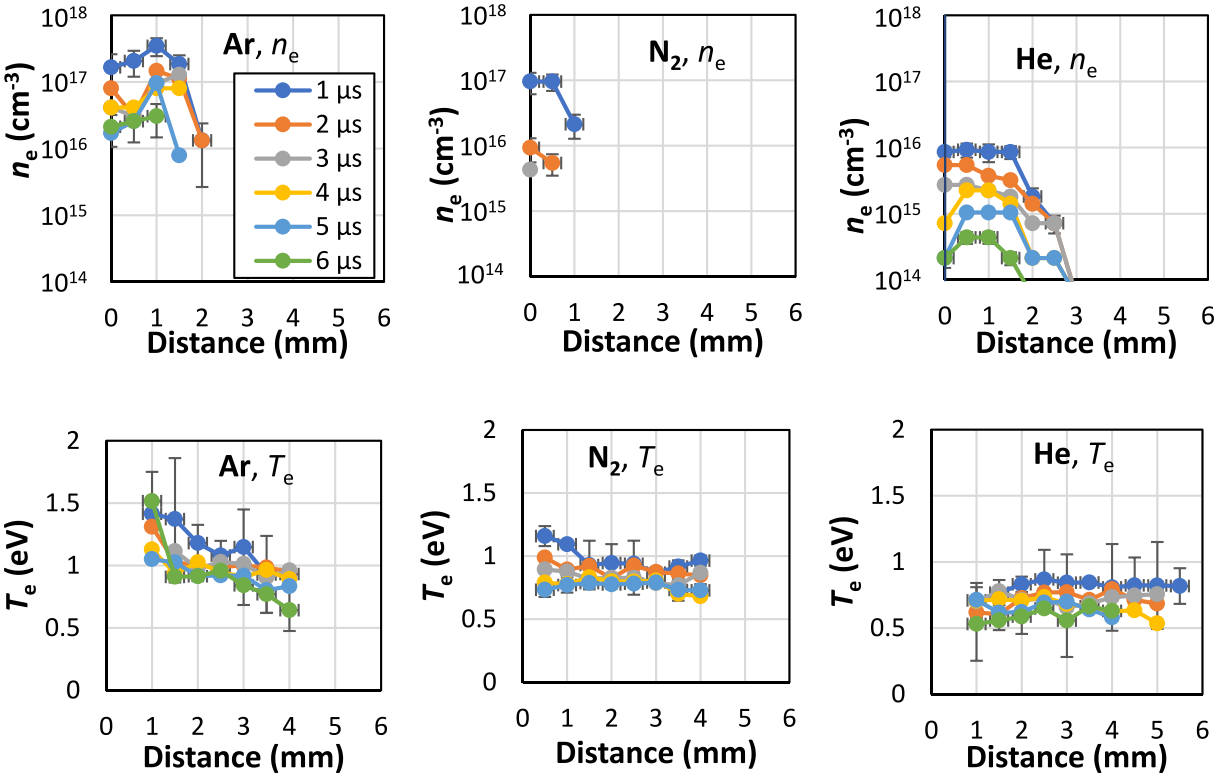

Fig. 7. The electron density (n_e) and electron temperature (T_e) according to atomic state distribution function (ASDF) of Mo I lines in the energy range of 3.2 to 5.6 eV as a function of distance from the target along the plume axis for different delay times in Ar, N_2 and He.

decreased quickly with the delay time. The extent of the high electron density region was the smallest in N_2. The electron density was smallest in He atmosphere and largest in Ar atmosphere. The result is consistent with the trends in the background emission which appears to be highest at the distance with the highest gradient of electron density.

The electron temperature was assumed to be equal to the atomic state distribution function (ASDF) of Mo I lines which was determined from the Boltzmann plot in the wavelength region of 644 to 665 nm (encompassing energies between 3.2 and 5.6 eV) similarly with our previous study [5]. The temperature could only be reliably determined at the distances where Mo line intensities were sufficiently strong. In all gases, the electron temperature decreased with time but the values and spatial distribution varied considerably in different gases (Fig. 7). Similarly with the electron density, the highest temperature was observed in Ar and the lowest temperature in He atmosphere consistently with earlier studies [6,7,20]. The temperature decreased in argon, was nearly constant in nitrogen and slightly increased in helium with increasing distances from the target. The increase may be explainable by stronger blast wave and subsequent faster diffusion of plasma in the He. In the case of N_2, the lower temperature can be explained by energy losses due to nitrogen dissociation and excitation of vibrational and rotational states [8,21]. In the case of He, the plume expands faster and also cools faster because of higher heat conduction and diffusion [9,22,23].

4. Summary and conclusions

The study investigated the temporal and spatial development of H_α and Mo line intensities and plasma parameters in the laser-induced plasma plume in Ar, N_2 and He at atmospheric pressure. Both the H_α line intensity and linewidth decreased fastest in the He atmosphere. The comparison of the line intensities at the same linewidth showed that the use of He atmosphere would allow considerably easier separation of the lines of hydrogen isotopes at atmospheric pressure compared to the use of Ar or N_2. However, it should be noted that the use of He atmosphere interferes with measuring He retention in the plasma-facing components. In such case, the Ar would be preferable to N_2 due to higher intensities at the same FWHM values. For 'in situ' LIBS analysis in the reactor vessel, the required gas atmosphere could be obtained by flushing the ambient environment with the desired gas.

The emission intensity of H_α and Mo I lines had different spatial distribution of intensity along the plasma plume which was at least partially caused by varying spatial distribution of plasma plume electron density and temperature. The electron density was highest near the target while the temperature distribution depended on the used gas atmosphere. The spatial variation of plasma parameters and line intensities has implications to the application of calibration-free LIBS which requires uniformity of plasma parameters. In the LIBS configuration which collects light perpendicularly with the target surface, expectedly used in remote-handling applications, the emission is simultaneously collected from different regions of the plasma plume with different plasma parameters. It allows to obtain strong signals from both H_α and metal lines but the determined electron temperature and density do not correspond to the same plasma region. Therefore, it is necessary to find LIBS parameters which improve the spatial uniformity of the plasma plume.

CRediT authorship contribution statement

Indrek Jõgi: Writing – original draft, Writing – review & editing, Formal analysis, Supervision, Project administration. **Jasper Ristkok:** Investigation, Writing – review & editing. **Jelena Butikova:** Investigation, Writing – review & editing. **Jüri Raud:** Investigation, Writing – review & editing. **Peeter Paris:** Conceptualization, Methodology, Investigation, Writing – review & editing, Supervision.

Declaration of Competing Interest

The authors declare that they have no known competing financial interests or personal relationships that could have appeared to influence the work reported in this paper.

Data availability

Data will be made available on request.

Acknowledgements

This work has been carried out within the framework of the EUROfusion Consortium, funded by the European Union via the Euratom Research and Training Programme (Grant Agreement No 101052200—EUROfusion). Views and opinions expressed are however those of the author(s) only and do not necessarily reflect those of the European Union or the European Commission. Neither the European Union nor the European Commission can be held responsible for them.

Institute of Solid State Physics, University of Latvia as the Center of Excellence has received funding from the European Union's Horizon 2020 Framework Programme H2020-WIDESPREAD-01-2016-2017-TeamingPhase2 under grant agreement No. 739508, project CAMART2.

References

[1] G. De Temmerman, M.J. Baldwin, D. Anthoine, K. Heinola, A. Jan, I. Jepu, J. Likonen, C.P. Lungu, C. Porosnicu, R.A. Pitts, Efficiency of thermal outgassing for tritium retention measurement and removal in ITER, Nucl. Mater. Energy. 12 (2017) 267–272, https://doi.org/10.1016/j.nme.2016.10.016.

[2] H.J. Van Der Meiden, S. Almaviva, J. Butikova, V. Dwivedi, P. Gasior, W. Gromelski, A. Hakola, X. Jiang, I. Jõgi, J. Karhunen, M. Kubkowska, M. Laan, G. Maddaluno, A. Marín-Roldán, P. Paris, K. Piip, M. Pisarčík, G. Sergienko, M. Veis, P. Veis, S. Brezinsek, Monitoring of tritium and impurities in the first wall of fusion devices using a LIBS based diagnostic, Nucl. Fusion 61 (2021), 125001, https://doi.org/10.1088/1741-4326/ac31d6.

[3] P. Paris, J. Butikova, M. Laan, M. Aints, A. Hakola, K. Piip, I. Tufail, P. Veis, Detection of deuterium retention by LIBS at different background pressures, Phys. Scr. T170 (2017), 014003.

[4] E.J. Kautz, E.C.E. Rönnebro, A. Devaraj, D.J. Senor, S.S. Harilal, Detection of hydrogen isotopes in Zircaloy-4: Via femtosecond LIBS, J. Anal. At. Spectrom 36 (2021) 1217–1227, https://doi.org/10.1039/d1ja00034a.

[5] I. Jõgi, J. Ristkok, J. Raud, J. Butikova, K. Mizohata, P. Paris, Laser induced breakdown spectroscopy for hydrogen detection in molybdenum at atmospheric pressure mixtures of argon and nitrogen, Fusion Eng. Des. 179 (2022), https://doi.org/10.1016/j.fusengdes.2022.113131.

[6] J.A. Aguilera, C. Aragón, A comparison of the temperatures and electron densities of laser-produced plasmas obtained in air, argon, and helium at atmospheric pressure, Appl. Phys. A Mater. Sci. Process. 69 (1999) 475–478, https://doi.org/10.1007/s003390051443.

[7] N. Farid, H. Wang, C. Li, X. Wu, H.Y. Oderji, H. Ding, G.N. Luo, Effect of background gases at reduced pressures on the laser treated surface morphology, spectral emission and characteristics parameters of laser produced Mo plasmas, J. Nucl. Mater. 438 (2013) 183–189, https://doi.org/10.1016/j.jnucmat.2013.03.022.

[8] A. De Giacomo, M. Dell'Aglio, R. Gaudiuso, S. Amoruso, O. De Pascale, Effects of the background environment on formation, evolution and emission spectra of laser-induced plasmas, Spectrochim Acta - Part B at. Spectrosc. 78 (2012) 1–19, https://doi.org/10.1016/j.sab.2012.10.003.

[9] E.J. Kautz, A. Devaraj, D.J. Senor, S.S. Harilal, Hydrogen isotopic analysis of nuclear reactor materials using ultrafast laser-induced breakdown spectroscopy, Opt. Express 29 (2021) 4936, https://doi.org/10.1364/oe.412351.

[10] S. Almaviva, L. Caneve, F. Colao, G. Maddaluno, R. Fantoni, Accessory laboratory measurements to support quantification of hydrogen isotopes by in-situ LIBS from a robotic arm inside a fusion vessel, Spectrochim Acta - Part B at. Spectrosc. 181 (2021), 106230, https://doi.org/10.1016/j.sab.2021.106230.

[11] A. Ciucci, V. Palleschi, S. Rastelli, A. Salvetti, D.P. Singh, E. Tognoni, CF-LIPS: A new approach to LIPS spectra analysis, Laser Part. Beams 17 (1999) 793–797, https://doi.org/10.1017/s0263034699174251.

[12] E. Tognoni, G. Cristoforetti, S. Legnaioli, V. Palleschi, Calibration-free laser-induced breakdown spectroscopy: state of the art, Spectrochim Acta - Part B at. Spectrosc. 65 (2010) 1–14, https://doi.org/10.1016/j.sab.2009.11.006.

[13] G. Cristoforetti, A. De Giacomo, M. Dell'Aglio, S. Legnaioli, E. Tognoni, V. Palleschi, N. Omenetto, Local thermodynamic equilibrium in laser-induced breakdown spectroscopy: beyond the McWhirter criterion, Spectrochim Acta - Part B at. Spectrosc. 65 (2010) 86–95, https://doi.org/10.1016/j.sab.2009.11.005.

[14] H. Suyanto, Z.S. Lie, H. Niki, K. Kagawa, K. Fukumoto, H. Rinda, S.N. Abdulmadjid, A.M. Marpaung, M. Pardede, M.M. Suliyanti, A.N. Hidayah, E. Jobiliong, T.J. Lie, M.O. Tjia, K.H. Kurniawan, Quantitative analysis of deuterium in zircaloy using double-pulse laser-induced breakdown spectrometry (LIBS) and helium gas plasma without a sample chamber, Anal. Chem. 84 (2012) 2224–2231, https://doi.org/10.1021/ac202744r.

[15] S. Almaviva, L. Caneve, F. Colao, V. Lazic, G. Maddaluno, P. Mosetti, A. Palucci, A. Reale, P. Gasior, W. Gromelski, M. Kubkowska, LIBS measurements inside the FTU vessel mock-up by using a robotic arm, Fusion Eng. Des. 157 (2020), 111685, https://doi.org/10.1016/j.fusengdes.2020.111685.

[16] L. Mercadier, J. Hermann, C. Grisolia, A. Semerok, Plume segregation observed in hydrogen and deuterium containing plasmas produced by laser ablation of carbon fiber tiles from a fusion reactor, Spectrochim Acta - Part B at. Spectrosc. 65 (2010) 715–720, https://doi.org/10.1016/j.sab.2010.04.011.

[17] I. Jõgi, P. Paris, J. Kozlova, H. Mändar, M. Passoni, D. Dellasega, A. Hakola, H.J. van der Meiden, LIBS study of ITER relevant tungsten-oxygen coatings exposed to deuterium plasma in Magnum-PSI, J. Nucl. Mater. In Press (2020) 152660.

[18] M.A. Gigosos, M.A. Gonzalez, V. Cadenoso, Computer simulated Balmer-alpha, -beta and -gamma Stark line profiles for non-equilibrium plasma diagnostics, Spectrochim Acta - Part B at. Spectrosc. 58 (2003) 1489–1504, https://doi.org/10.1016/S0584-8547.

[19] A. De Giacomo, R. Gaudiuso, M. Dell'Aglio, A. Santagata, The role of continuum radiation in laser induced plasma spectroscopy, Spectrochim Acta - Part B at. Spectrosc. 65 (2010) 385–394, https://doi.org/10.1016/j.sab.2010.03.016.

[20] S. Khan, S. Bashir, A. Hayat, M. Khaleeq-Ur-Rahman, F.U. Haq, Laser-induced breakdown spectroscopy of tantalum plasma, Phys. Plasmas 20 (2013), 073104, https://doi.org/10.1063/1.4812451.

[21] A.R. Casavola, G. Colonna, M. Capitelli, Kinetic model of titanium laser induced plasma expansion in nitrogen environment, Plasma Sources Sci. Technol. 18 (2009), 025027, https://doi.org/10.1088/0963-0252/18/2/025027.

[22] S.B. Wen, X. Mao, R. Greif, R.E. Russo, Laser ablation induced vapor plume expansion into a background gas. II. Experimental analysis, J. Appl. Phys. 101 (2007), https://doi.org/10.1063/1.2431085.

[23] S.V. Shabanov, I.B. Gornushkin, Two-dimensional axisymmetric models of laser induced plasmas relevant to laser induced breakdown spectroscopy, Spectrochim Acta - Part B at. Spectrosc. 100 (2014) 147–172, https://doi.org/10.1016/j.sab.2014.08.026.